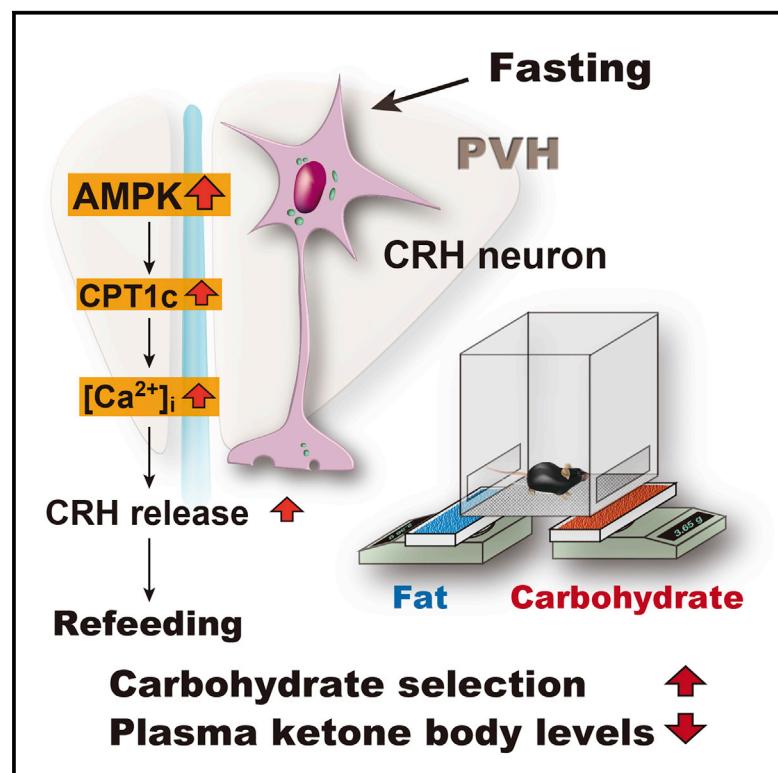


## Activation of AMPK-Regulated CRH Neurons in the PVH is Sufficient and Necessary to Induce Dietary Preference for Carbohydrate over Fat

### Graphical Abstract



### Authors

Shiki Okamoto, Tatsuya Sato, Michihiro Tateyama, ..., Toshihiko Yada, Barbara B. Kahn, Yasuhiko Minokoshi

### Correspondence

minokosh@nips.ac.jp

### In Brief

Food selection is influenced by nutritional state as well as food palatability. However, the mechanism remains unknown. Okamoto et al. find that activation of an AMPK-CPT1c pathway in a subset of CRH-positive neurons in the paraventricular hypothalamus mediates the fasting-induced increase in high-carbohydrate diet selection.

### Highlights

- AMPK in a subset of CRH neurons in the PVH is preferentially activated by fasting
- AMPK activation in CRH neurons promotes selection of carbohydrates over fat
- CPT1c in CRH neurons is necessary for AMPK- or fasting-induced carbohydrate selection
- Carbohydrate feeding after fasting quickly decreases plasma ketone body levels



# Activation of AMPK-Regulated CRH Neurons in the PVH is Sufficient and Necessary to Induce Dietary Preference for Carbohydrate over Fat

Shiki Okamoto,<sup>1,2,3</sup> Tatsuya Sato,<sup>1,2</sup> Michihiro Tateyama,<sup>2,4</sup> Haruaki Kageyama,<sup>5</sup> Yuko Maejima,<sup>6,16</sup> Masanori Nakata,<sup>6</sup> Satoshi Hirako,<sup>7</sup> Takashi Matsuo,<sup>1,8</sup> Sanda Kyaw,<sup>1,9</sup> Tetsuya Shiuchi,<sup>1,17</sup> Chitoku Toda,<sup>1,18</sup> Udval Sedbazar,<sup>6</sup> Kumiko Saito,<sup>1</sup> Nur Farehan Asgar,<sup>1,2</sup> Boyang Zhang,<sup>6</sup> Shigefumi Yokota,<sup>1,19</sup> Kenta Kobayashi,<sup>2,10</sup> Fabienne Fougelle,<sup>11,12,13</sup> Pascal Ferré,<sup>11,12,13</sup> Masamitsu Nakazato,<sup>8</sup> Hiroaki Masuzaki,<sup>3</sup> Seiji Shioda,<sup>14</sup> Toshihiko Yada,<sup>6</sup> Barbara B. Kahn,<sup>15</sup> and Yasuhiko Minokoshi<sup>1,2,20,\*</sup>

<sup>1</sup>Division of Endocrinology and Metabolism, Department of Homeostatic Regulation, National Institute for Physiological Sciences, National Institute of Natural Sciences, 38 Nishigonaka, Myodaiji, Okazaki, Aichi 444-8585, Japan

<sup>2</sup>Department of Physiological Sciences, School of Life Science, SOKENDAI (The Graduate University for Advanced Studies), 38 Nishigonaka, Myodaiji, Okazaki, Aichi 444-8585, Japan

<sup>3</sup>Second Department of Internal Medicine (Endocrinology, Diabetes and Metabolism, Hematology, Rheumatology), Graduate School of Medicine, University of the Ryukyus, 207 Uehara, Nishihara, Nakagami-gun, Okinawa 903-0215, Japan

<sup>4</sup>Division of Biophysics and Neurobiology, Department of Molecular and Cellular Physiology, National Institute for Physiological Sciences, National Institute of Natural Sciences, 38 Nishigonaka, Myodaiji, Okazaki, Aichi 444-8585, Japan

<sup>5</sup>Department of Nutrition, Faculty of Health Care, Kiryu University, 606-7 Kasakake-cho Azami, Midori, Gunma 379-2392, Japan

<sup>6</sup>Division of Integrative Physiology, Department of Physiology, Jichi Medical University School of Medicine, 3311-1 Yakushiji, Shimotsuke, Tochigi 329-0498, Japan

<sup>7</sup>Department of Health and Nutrition, University of Human Arts and Sciences, 1288 Magome, Iwatsuki-ku, Saitama-shi, Saitama 339-8539, Japan

<sup>8</sup>Division of Neurology, Respiratory, Endocrinology, and Metabolism, Department of Internal Medicine, University of Miyazaki, 5200 Kihara, Kiyotake, Miyazaki 889-1692, Japan

<sup>9</sup>Department of Physiology, University of Medicine 1, Yangon, Myanmar

<sup>10</sup>Section of Viral Vector Development, National Institute for Physiological Sciences, National Institute of Natural Sciences, 38 Nishigonaka, Myodaiji, Okazaki, Aichi 444-8585, Japan

<sup>11</sup>Sorbonne Universités, UPMC Univ Paris 06, UMR\_S 1138, Centre de Recherche des Cordeliers, F-75006 Paris, France

<sup>12</sup>INSERM, UMR\_S 1138, Centre de Recherche des Cordeliers, F-75006 Paris, France

<sup>13</sup>Université Paris Descartes, Sorbonne Paris Cité, UMR\_S 1138, Centre de Recherche des Cordeliers, F-75006 Paris, France

<sup>14</sup>Division of Peptide Drug Innovation, Global Research Center for Innovative Life Science, Hoshi University School of Pharmacy and Pharmaceutical Sciences, 2-4-41 Ebara, Shinagawa-ku, Tokyo 142-8501, Japan

<sup>15</sup>Division of Endocrinology, Diabetes, and Metabolism, Department of Medicine, Beth Israel Deaconess Medical Center and Harvard Medical School, Boston, MA 02215, USA

<sup>16</sup>Present address: Department of Pharmacology, Fukushima Medical University School of Medicine, 1 Hikarigaoka, Fukushima 960-1295, Japan

<sup>17</sup>Present address: Department of Integrative Physiology, Tokushima University Graduate School, 3-18-15 Kuramoto, Tokushima, Tokushima 770-8503, Japan

<sup>18</sup>Present address: Department of Biomedical Sciences, Graduate School of Veterinary Medicine, Hokkaido University, Kita 18, Nishi 9, Kita-ku, Sapporo, Hokkaido 060-0818, Japan

<sup>19</sup>Present address: Department of Endocrinology, Metabolism and Hypertension, Clinical Research Institute, National Hospital Organization, Kyoto Medical Center, 1-1 Mukaihata-cho, Fukakusa, Fushimi-ku, Kyoto 612-8555 Japan

<sup>20</sup>Lead Contact

\*Correspondence: [minokosh@nips.ac.jp](mailto:minokosh@nips.ac.jp)  
<https://doi.org/10.1016/j.celrep.2017.11.102>

## SUMMARY

Food selection is essential for metabolic homeostasis and is influenced by nutritional state, food palatability, and social factors such as stress. However, the mechanism responsible for selection between a high-carbohydrate diet (HCD) and a high-fat diet (HFD) remains unknown. Here, we show that activation of a subset of corticotropin-releasing hormone (CRH)-positive neurons in the rostral region of the paraventricular hypothalamus (PVH) induces selection of an

HCD over an HFD in mice during refeeding after fasting, resulting in a rapid recovery from the change in ketone metabolism. These neurons manifest activation of AMP-activated protein kinase (AMPK) during food deprivation, and this activation is necessary and sufficient for selection of an HCD over an HFD. Furthermore, this effect is mediated by carnitine palmitoyltransferase 1c (CPT1c). Thus, our results identify the specific neurons and intracellular signaling pathway responsible for regulation of the complex behavior of selection between an HCD and an HFD.



## INTRODUCTION

The preference for a high-fat diet (HFD) among multiple palatable diets has increased in the modern world (Mann, 2002), whereas carbohydrate craving is often induced by stressful life events and mood disturbances (Roberts et al., 2014; Rutters et al., 2009). In rodents, they often cause a craving of sucrose drinking, which is regulated by the reward system, including dopamine release in the striatum (Tellez et al., 2016). Some strains of rodents are also hyperphagic when fed an HFD *ad libitum*. However, food selection is influenced by nutritional state as well as food palatability. When rodents are re-fed after fasting, they select a high-carbohydrate diet (HCD) over an HFD (Hunsicker et al., 1992; Welch et al., 1994). The neural mechanism for the selection between an HCD and an HFD after food deprivation remains elusive and is of high importance in light of the current obesity epidemic.

The evolutionarily conserved serine-threonine kinase AMPK (AMP-activated protein kinase) functions as a metabolic sensor that regulates fatty acid oxidation (FAO) via changes in acetyl-coenzyme A (acetyl-CoA) carboxylase (ACC) and carnitine palmitoyltransferase 1 (CPT1) activity and related gene expression (Hardie, 2007). AMPK in the mediobasal hypothalamus plays an important role in the control of total calorie intake by responding to hormonal and nutrient signals (Andrews et al., 2008; Minokoshi et al., 2004). AMPK in the paraventricular hypothalamus (PVH) and the mediobasal hypothalamus is activated by fasting in mice (Minokoshi et al., 2004). The PVH also plays a role in macronutrient selection (Leibowitz, 1995). The fatty acid synthase (FAS) inhibitor C75, which alters metabolism in the brain and peripheral tissues, suppresses AMPK activity in the brain (Kim et al., 2004) as well as food intake (Kim et al., 2004; Loftus et al., 2000). However, the anorexic effect of FAS inhibition is apparent when mice are fed standard laboratory chow, but not when they are fed a low-carbohydrate (ketogenic) diet (Wortman et al., 2003). Thus, although AMPK has been believed as a “metabolic sensor” that controls total calorie intake, the AMPK pathway in the brain may also regulate selection between carbohydrates and fat.

Here, we show that a subset of corticotropin-releasing hormone (CRH)-positive neurons in the PVH plays a central role in selection between carbohydrate- and fat-enriched diets via activation of AMPK and CPT1c, the neuronal isoform of CPT1. Our data thus uncover a function of AMPK and CRH neurons in the regulation of food preference.

## RESULTS

### Activation of AMPK in the PVH Promotes HCD Selection

AMPK in the arcuate nucleus of the hypothalamus (ARH) is essential to activate AgRP neurons in the nucleus during fasting (Andrews et al., 2008), whereas the regulatory role of AMPK in the PVH in food intake remains unknown. We injected male C57BL/6J mice bilaterally in the PVH with lentivirus encoding either a constitutively active (CA) form of AMPK (truncated rat  $\alpha$ 1 subunit [amino acids 1–312], with Thr<sup>172</sup> replaced by Asp) (Woods et al., 2000) or EGFP, each under the control of the synapsin 1 gene promoter (Figure S1A). The FLAG-epitope-tagged CA-AMPK protein was largely restricted to the PVH after infec-

tion, and CA-AMPK mRNA was detected at 1 and 3 months after infection (Figure 1A). Fluorescence microscopy revealed that EGFP was expressed in the PVH and nearby regions around the nucleus (Figure 1B). EGFP was coexpressed with the endogenous neuron-specific marker NeuN in the PVH (Figure 1B). Mice expressing CA-AMPK (CA-AMPK mice) manifested an increased amount of phosphorylated (p) ACC in the PVH (and nearby regions around the PVH), but not in the ARH or parietal cortex, compared with EGFP mice (Figure 1C).

CA-AMPK mice gained more weight than EGFP mice when maintained on normal lab chow. However, unexpectedly, they gained less weight than the control animals when fed an HFD (Figure 1D). We examined calorie intake in CA-AMPK mice maintained on three different diets: lab chow, HCD1, and HFD1 (Table S1). Although body weight was not statistically different between CA-AMPK and control mice at 1 month after virus infection (Figure 1D), total caloric intake in CA-AMPK mice was increased when the animals were fed lab chow or HCD1, but it was decreased when they were fed HFD1, compared with EGFP mice (Figure 1E). These differences in calorie intake were attributable to differences in food intake predominantly during the dark period (Figure S1B). Energy expenditure did not differ between CA-AMPK and control mice maintained on lab chow at 1 month after virus infection (Figure S1C). These results indicated that expression of CA-AMPK in neurons in the PVH and nearby regions around the nucleus increased the intake of HCD1 but attenuated that of HFD1 and that the increased body weight of chow-fed CA-AMPK mice was the result of increased calorie intake. Activation of CRH neurons in the PVH has been reported to increase thermogenesis in BAT (brown adipose tissue) (Cheng et al., 2011). However, UCP1 (uncoupling protein 1)-knockout mice do not change body weight below the thermo-neutral room temperature (Enerbäck et al., 1997). Thus, whole-body energy expenditure might not be affected even if BAT thermogenesis is suppressed in CA-AMPK mice.

To further explore the effect of CA-AMPK expression in the PVH on food selection behavior, we performed a two-diet choice experiment with HCD1 and HFD1 (Figure 1F). Under the condition of *ad libitum* feeding, HCD1 intake was increased and HFD1 intake was decreased in CA-AMPK mice compared with EGFP mice (Figure 1G). Analysis of macronutrient (carbohydrate, fat, and protein) intake calculated from the composition of HFD1 and HCD1 (Table S1) revealed that carbohydrate intake was increased and fat intake was reduced in CA-AMPK mice, whereas protein intake did not differ between the two groups of mice (Figure 1G). Total calorie intake was unchanged in CA-AMPK mice compared with EGFP mice, since control mice fed *ad libitum* also increased total calorie intake in two-diet choice experiments (Figure 1G).

We examined food selection with different combinations of diets (Tables S1 and S2). HFD1 and HCD1 consisted of different ingredients such as minerals as well as different dietary fat and carbohydrate (Table S1). To examine whether CA-AMPK mice choose HCD1 over HFD1 when the only difference is dietary fat and carbohydrate and not other ingredients, we next examined selection between HFD2 and HCD2. HFD2 and HCD2 consisted of the same dietary carbohydrate and fat as HFD1 and HCD1, respectively, but other ingredients were replaced

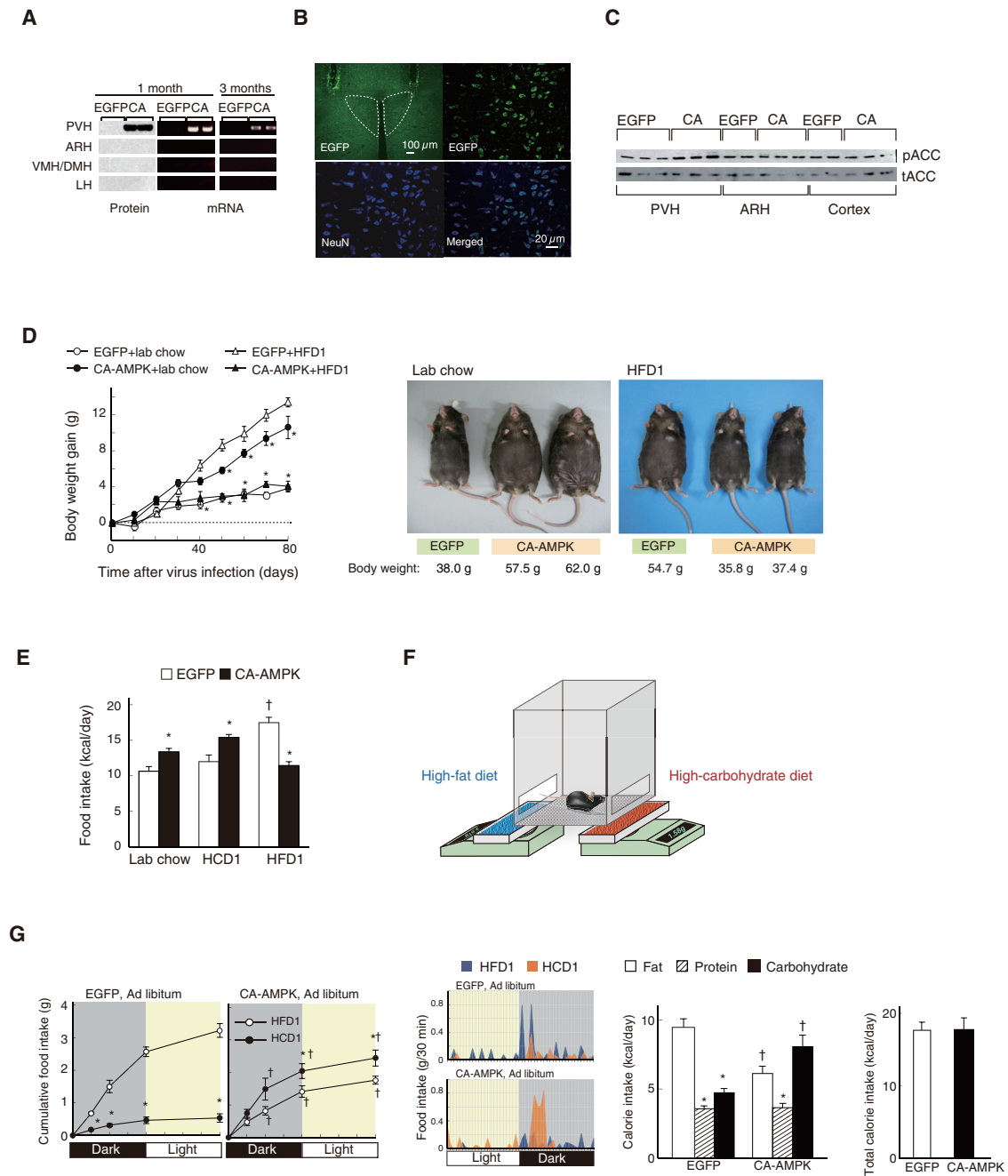


**Figure 1. Expression of CA-AMPK in PVH Neurons Promotes HCD Selection and Induces Obesity in Mice Fed an HCD, but Not an HFD**  
 (A) Immunoblot analysis of CA-AMPK (CA) protein and RT-PCR analysis of CA-AMPK mRNA in hypothalamic nuclei of CA-AMPK or control (EGFP) mice at 1 or 3 months after lentiviral infection.  
 (B) EGFP fluorescence (green) and NeuN immunofluorescence staining (blue) in brain sections of EGFP-expressing control mice. The top left panel shows bilateral expression of EGFP in the PVH (outlined with dashed lines). Higher-magnification views of the boxed region show individual cells expressing EGFP (top right) or NeuN (bottom left) as well as a merged image (bottom right). Scale bars represent 100 and 20  $\mu$ m, respectively.  
 (C) Immunoblot analysis of Ser<sup>79</sup>-phosphorylated (p) and total (t) forms of ACC in the PVH, ARH, or parietal cortex of CA-AMPK or EGFP mice maintained on lab chow for 4 weeks after virus infection.  
 (D) Body weight changes of CA-AMPK and EGFP mice maintained on lab chow or HFD1. Body weights at time 0 (1 week after infection) were as follows: EGFP + lab chow, 26.1  $\pm$  0.59 g; CA-AMPK + lab chow, 25.6  $\pm$  0.24 g; EGFP + HFD1, 25.1  $\pm$  0.73 g; and CA-AMPK + HFD1, 27.1  $\pm$  0.81 g (not significantly different). Photos show representative EGFP and CA-AMPK mice fed lab chow or HFD1 for 6 months after virus infection. Data represent means  $\pm$  SEM (n = 6). \*p < 0.05 versus corresponding value for EGFP mice fed the same diet.  
 (E) Food intake (kcal/day) for EGFP and CA-AMPK mice on lab chow, HCD1, and HFD1.  
 (F) Schematic of the diet selection apparatus.  
 (G) Cumulative food intake (g) and food intake (g/30 min) for EGFP and CA-AMPK mice on HFD1 and HCD1. Bar graphs show calorie intake (kcal/day) and total calorie intake (kcal/day).

(legend continued on next page)

with those of HCD1 and HFD1, respectively (Table S1). We also examined food selection with different combinations of diets derived from distinct sources that controlled for vitamin and mineral content (Table S2): HFD1 (lard) versus HCD3 (sucrose), HFD1 (lard) versus HCD4 (cornstarch), HFD3 (coconut oil) versus HCD5 (sucrose), and HFD3 (coconut oil) versus HCD6 (cornstarch). In two-diet choice experiments, CA-AMPK mice showed increased selection of each HCD and decreased selection of the HFD regardless of source, without a change in total calorie intake (Figure S1D). When presented with individual diets, CA-AMPK mice showed increased intake of HCDs and reduced intake of HFDs compared with EGFP mice (Figure S1E). Together, these results showed that whereas EGFP mice preferred mostly HFDs, CA-AMPK mice increased intake of HCDs and reduced that of HFDs, and this selection of carbohydrate over fat did not result from a preference for other nutrients or ingredients in the diets.

### Food Deprivation Promotes HCD Selection via AMPK and CPT1c

To examine the physiological relevance of CA-AMPK-induced selection of HCD over HFD, we next examined the effect of food deprivation on selection between HFD1 and HCD1 during refeeding. Rodents increase carbohydrate intake during refeeding after fasting (Hunsicker et al., 1992; Welch et al., 1994). AMPK in the PVH of mice is activated by food deprivation for 24 hr (Minokoshi et al., 2004). Food deprivation overnight increased phosphorylation of  $\alpha$ AMPK and ACC in the PVH compared with the refed state (lab chow) (Figure 2A; see also Figure S2B for validation of the antibodies to pAMPK for immunohistochemistry). The activity of  $\alpha$ 2AMPK in the PVH was also increased after overnight food deprivation compared with refeeding (Figure 2B). The activity of  $\alpha$ 2AMPK in the PVH in mice fed *ad libitum* was within the range of the activity between fasting and refeeding (data not shown). The suppression of  $\alpha$ 2AMPK activity was greater in mice refed with lab chow or HCD1 than in those refed with HFD1.

A two-diet choice experiment revealed that mice deprived of food for ~24 hr (17:30 to 18:00 on the next day) (1) selected HCD1 over HFD1 during the initial 3 hr of refeeding, (2) showed a marked reduction in HFD1 consumption after this period, and (3) maintained selection of HCD1 versus HFD1 over 24 hr (Figure 2C). Mice fed *ad libitum* chose mostly HFD1. Most mice first fed on HFD1 before switching to HCD1 during the initial 3 hr of refeeding, which is consistent with the previous observation that rats select fat over carbohydrate during the initial 1-hr period after fasting (Hunsicker et al., 1992). These data suggest that the preference for an HFD is maintained after fasting (see representative profile of food selection in Figure 2C). Analysis

of macronutrient intake revealed that fasting increased carbohydrate intake and reduced fat intake, with no change in protein intake, compared with *ad libitum* feeding (Figure 2C). Total calorie intake during 24 hr of refeeding did not differ from that during *ad libitum* feeding (Figure 2C).

We next examined food selection with different combinations of diets: HFD2 versus HCD2 (Table S1) and HFD1 versus HCD3 (Table S2). Compared with mice fed *ad libitum*, fasted mice increased intake of either HCD and reduced that of the HFD, without a change in total calorie intake, during refeeding in two-diet choice experiments (Figures S1F and S1G). These results suggested that fasted mice increase selection of carbohydrate and reduce that of fat, without a change in preference for other nutrients or ingredients in the presented diets. Food deprivation thus activates AMPK in the PVH and increases selection of carbohydrate over fat during refeeding.

To explore the mechanism by which AMPK activation in the PVH and food deprivation affect food selection, we examined changes in gene expression. AMPK regulates FAO in mitochondria via upregulation of CPT1 activity and gene expression (Hardie, 2007; López et al., 2008). qRT-PCR analysis showed that expression of CA-AMPK in the PVH increased the expression of FAO-related genes including those for CPT1a, the neuronal CPT1 isoform CPT1c (Dai et al., 2007), fatty acid transport protein 1 (FATP1), and uncoupling protein 2 (UCP2) in this brain region (Andrews et al., 2008) (Figure 2D). Fasting also increased the expression of these genes in the PVH compared with that apparent at 6 hr after refeeding with lab chow (Figure 2E). CPT1b mRNA was not detected in the PVH (data not shown). These results suggested that AMPK activation increases expression of FAO-related genes in the PVH.

FAO measured *ex vivo* was also increased in the PVH of EGFP mice during fasting compared with that apparent at 3 h after refeeding with lab chow (Figure 2F). FAO was also increased in the PVH of CA-AMPK mice compared with EGFP mice during refeeding (Figure 2F). Treatment with etomoxir, which inhibits CPT1 activity through formation of etomoxiryl-coenzyme A (etomoxiryl-CoA) (which mimics malonyl-coenzyme A [malonyl-CoA]) (Bentebibel et al., 2006), prevented the increase in FAO in the PVH induced by overnight fasting or expression of CA-AMPK (Figure 2F). Thus, fasting and CA-AMPK expression in PVH neurons each increases FAO in the PVH.

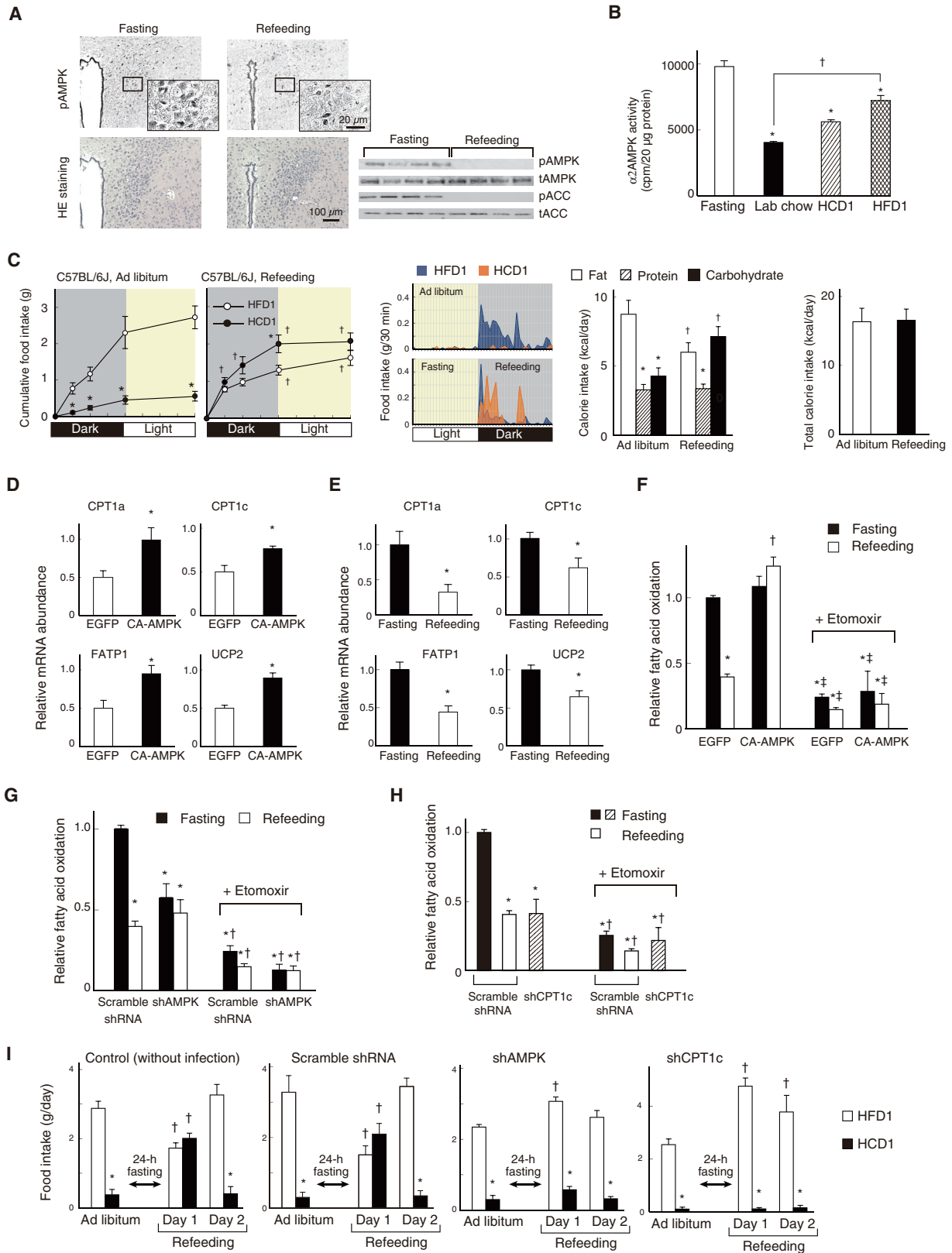
To examine whether fasting increases FAO in the PVH through activation of AMPK and CPT1c, we knocked down AMPK or CPT1c in the PVH (Figure S2A). Expression of a short hairpin RNA (shRNA) specific for  $\alpha$ 1 and  $\alpha$ 2 subunits of AMPK reduced the abundance of the corresponding mRNAs and suppressed the increase in pAMPK induced by the AMPK activator AICAR (5-aminoimidazole-4-carboxamide-1- $\beta$ -D-ribofuranoside)

(E) Caloric intake of CA-AMPK or EGFP mice fed lab chow, HCD1, or HFD1 alone. Data represent means  $\pm$  SEM ( $n = 6$ ). \* $p < 0.05$  versus corresponding value for EGFP mice; † $p < 0.05$  versus value for EGFP mice fed lab chow. See also Figures S1B and S1C for profiles of food intake during a 24-hr period and for energy expenditure during light and dark periods, respectively, for these mice.

(F) Analytic cage for two-diet choice experiments with an HFD versus an HCD.

(G) Selection of HFD1 versus HCD1 in a two-diet choice experiment with CA-AMPK or EGFP mice. Cumulative food intake, representative profiles of food intake, macronutrient (carbohydrate, fat, and protein) intake, and 24-hr total calorie intake are shown from left to right. Data represent means  $\pm$  SEM ( $n = 6$ ). \* $p < 0.05$  versus corresponding value for HFD1 or fat intake; † $p < 0.05$  versus corresponding value for EGFP mice.

See also Tables S1 and S2 and Figure S1.



(legend on next page)

in C2C12 cells (Figure S2B). Expression of AMPK shRNA in the PVH of mice (shAMPK mice) also reduced the amounts of  $\alpha$ 1- and  $\alpha$ 2AMPK mRNAs (Figure S2C) and pAMPK in the PVH without affecting pAMPK abundance in the ARH or parietal cortex during fasting (Figure S2D). The fasting-induced increase in FAO in the PVH was also blunted in shAMPK mice (Figure 2G). Expression of an shRNA for CPT1c in the PVH of mice (shCPT1c mice) reduced the amount of CPT1c mRNA (but not that of CPT1a mRNA) (Figure S2E) and suppressed fasting-induced FAO (Figure 2H) in the PVH. The two-diet choice experiments revealed that knockdown of AMPK or CPT1c in the PVH inhibited the fasting-induced changes both in food selection between HCD1 and HFD1 and in macronutrient intake, whereas expression of a scrambled shRNA (scramble shRNA mice) did not affect these parameters compared with those apparent for noninfected control mice (Figures 2I and S2F). Both shAMPK and shCPT1c mice thus showed a significant increase in HFD1 and dietary fat intake during refeeding compared with *ad libitum* feeding. Similarly, acute inhibition of CPT1 activity by bilateral injection of etomoxir into the PVH 30 min before refeeding blunted the fasting-induced changes in food selection (Figure S3A). Intraperitoneal (i.p.) or intracerebroventricular (i.c.v.) injection of glucose suppresses the fasting-induced activation of AMPK in the PVH (Minokoshi et al., 2004). The i.c.v. injection of glucose 30 min before refeeding inhibited the fasting-induced changes in food selection (Figure S3A). The CA-AMPK-induced selection of HCD1 over HFD1 during 24 hr was also blunted by etomoxir injection into the PVH at 30 min before the start of the dark period (Figure S3B). Etomoxir injection did not affect food selection in EGFP mice fed *ad libitum* (Figure S3B). These results thus suggested that activation of the AMPK-CPT1c axis in the PVH during fasting increases HCD selection and reduces HFD selection during refeeding.

To examine whether etomoxir alters the perception of sweet taste, we tested the effect of bilateral injection of etomoxir into the PVH on drinking of a saccharin solution. C57BL/6J mice

consumed a much larger amount of saccharin solution than water during the initial 3 hr after a 24-hr fast. Injection of etomoxir into the PVH did not change the amount of saccharin drunk (Figure S3C; Movie S1), whereas preconditioning with LiCl, an aversive unconditioned stimulus, suppressed saccharin drinking. The preference for a sweet taste thus remained intact after etomoxir injection into the PVH. These results suggested that sweet taste is unlikely the primary regulator of selection between an HCD and an HFD during refeeding after fasting. The increase in HCD selection during refeeding may instead be mediated by metabolic changes induced by food deprivation.

To test whether HCD selection during refeeding after fasting ameliorates the metabolic changes induced by fasting, we examined plasma ketone and glucose levels in mice presented with HFD1 or HCD3 alone. In contrast to the two-diet choice experiment, fasting increased intake of HFD1 more than that of HCD3 (Figure S3D). The preference for dietary fat was thus maintained after fasting for 24 hr. However, refeeding with HFD1 for 1 hr after fasting was associated with a higher plasma concentration of ketone bodies and a lower plasma glucose concentration compared with HCD3 refeeding (Figures S3E and S3F). The plasma concentration of ketone bodies did not decline when mice were pair-fed with the same number of calories in HFD1 as that consumed by mice refed with HCD3. These results suggested that HCD selection induced by activation of AMPK in PVH neurons results in a more rapid recovery from the changes in ketone and glucose metabolism induced by food deprivation compared with that observed during refeeding with an HFD. Mice thus likely increase HCD selection during refeeding in order to rapidly reverse the metabolic changes induced by food deprivation.

### CRH Neurons in the PVH Regulate Food Selection

To identify which neurons in the PVH and nearby regions are primarily responsible for regulation of food selection (HFD1 versus HCD1), we injected multiple neuropeptides or cytokines that are

#### Figure 2. Food Deprivation Increases HCD Selection via AMPK and CPT1c in the PVH

(A) Immunohistochemical staining of Thr<sup>172</sup>-phosphorylated  $\alpha$ AMPK (pAMPK) as well as H&E staining in the PVH of C57BL/6J mice after overnight fasting or subsequent refeeding for 3 hr with lab chow (left). Scale bar, 100  $\mu$ m. Insets show higher-magnification images of pAMPK-positive PVH neurons in the boxed regions; scale bar, 20  $\mu$ m. Right panel shows immunoblot analysis of Thr<sup>172</sup>-phosphorylated (p) and total (t) forms of  $\alpha$ AMPK as well as of Ser<sup>79</sup>-phosphorylated (p) and total (t) forms of ACC in the PVH.

(B)  $\alpha$ 2AMPK activity in the PVH of C57BL/6J mice after overnight fasting or refeeding with lab chow, HCD1, or HFD1 for 3 hr. Data represent means  $\pm$  SEM (n = 5 or 6). \*p < 0.05 versus fasting; †p < 0.05 for the indicated comparison.

(C) Food selection (HFD1 versus HCD1) in a two-diet choice experiment with C57BL/6J mice fed *ad libitum* or refed from the onset of the dark period following a 24-hr fast (17:30 to 18:00 on the next day). Cumulative food intake, representative profiles of food intake, macronutrient intake, and 24-hr total calorie intake are shown from left to right. Mice were maintained on lab chow until the experiment. Data represent means  $\pm$  SEM (n = 5). \*p < 0.05 versus corresponding value for HFD1 or fat intake; †p < 0.05 versus corresponding value for *ad libitum*.

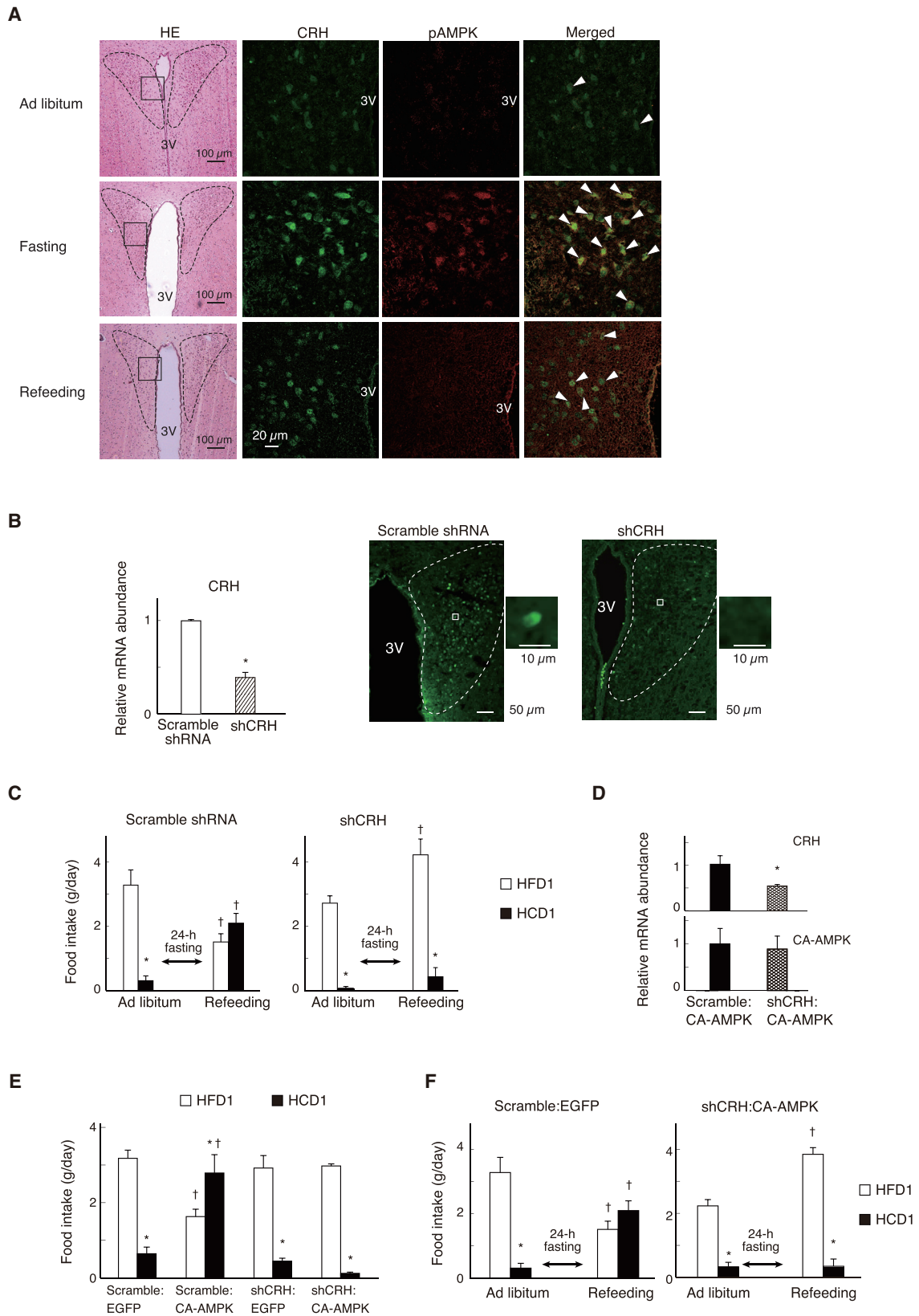
(D and E) RT-qPCR analysis of relative CPT1a, CPT1c, FATP1, and UCP2 mRNA abundance in the PVH of CA-AMPK or EGFP mice fed *ad libitum* (D) and of C57BL/6J mice after overnight fasting or subsequent refeeding for 6 hr with lab chow (E). Data represent means  $\pm$  SEM (n = 5). \*p < 0.05 versus EGFP control or fasting.

(F) Relative FAO measured *ex vivo* in the PVH of EGFP or CA-AMPK mice deprived of food overnight with or without refeeding with lab chow for 3 hr. Etomoxir was injected unilaterally into the PVH and present continuously in the incubation medium as indicated. Data represent means  $\pm$  SEM (n = 5). \*p < 0.05 versus fasting EGFP mice without etomoxir; †p < 0.05 versus corresponding value for EGFP mice without etomoxir; ‡p < 0.05 versus corresponding value for without etomoxir.

(G and H) Relative FAO measured *ex vivo* in the PVH of shAMPK or scramble shRNA control mice (G) and of shCPT1c or scramble shRNA mice (H) as in (F). Data represent means  $\pm$  SEM (n = 5 or 6). \*p < 0.05 versus fasting scramble shRNA mice without etomoxir; †p < 0.05 versus corresponding value for without etomoxir.

(I) Food selection (HFD1 versus HCD1) in a two-diet choice experiment with control (without infection), scramble shRNA, shAMPK, or shCPT1c mice before and after a 24-hr fast. Data are means  $\pm$  SEM (n = 6). \*p < 0.05 versus corresponding HFD1 value; †p < 0.05 versus corresponding value for before fasting. See also Figure S2F for macronutrient intake in the same mice.

See also Figures S1 to S3 and Movie S1.



(legend on next page)

expressed in PVH neurons into either the PVH or the lateral ventricle. Among these peptides and cytokines, only CRH injection into the PVH increased selection of HCD1 and reduced that of HFD1 without affecting total calorie intake over 24 hr (Figures S4A and S4B). Consistent with the notion that CRH neurons are responsible for this diet selection, immunofluorescence analysis revealed that overnight fasting increased the abundance of pAMPK mostly within CRH-positive neurons in the rostral region, but not in the caudal region, of the PVH (Figures 3A and S4C). The proportion of CRH neurons positive for pAMPK in the rostral region thus increased from 0% to ~30% (15/45 cells) after fasting. We found only a few CRH-negative, pAMPK-positive cells in the PVH after fasting (Figures S4C).

We next examined whether CRH in the PVH is necessary for HCD selection during refeeding after fasting. Bilateral injection of the CRH receptor 1 (CRHR1) antagonist antalarmin into the PVH attenuated the fasting-induced change in food selection between HFD1 and HCD1, with the treated mice showing increased HFD1 intake (Figure S5A). Injection of the vehicle (DMSO) had no such effect. These results suggested that both CRH neurons and CRHR1 in the PVH are necessary for the fasting-induced change in food selection. Lentivirus-mediated bilateral expression of a CRH shRNA (Figure S5B) in the PVH of mice (shCRH mice) reduced the amount of CRH mRNA in the PVH compared with that apparent in scramble shRNA mice (Figure 3B). The fasting-induced changes in food selection between HFD1 and HCD1 and in macronutrient intake were also attenuated in shCRH mice (Figures 3C and S5C).

To test whether CRH in the PVH is necessary for the effect of CA-AMPK expression in PVH neurons on food selection, we bilaterally injected lentiviruses encoding both CA-AMPK and either scrambled or CRH shRNAs (Figure S5D) into the PVH of mice to yield scramble:CA-AMPK and shCRH:CA-AMPK mice, respectively. Expression of the CRH shRNA reduced the abundance of CRH mRNA by ~50%, without affecting the abundance of CA-AMPK mRNA, in the PVH of shCRH:CA-AMPK mice (Figure 3D). The CA-AMPK-induced changes in food selection between HFD1 and HCD1 (Figure 3E) and macronutrient intake (Figure S5E) were blunted in shCRH:CA-AMPK mice. Further-

more, the effect of fasting on food selection was also attenuated in shCRH:CA-AMPK mice (Figure 3F). These results thus suggested that CRH in the PVH is necessary for both the fasting- and CA-AMPK-induced changes in food selection.

To explore whether activation or inhibition of CRH neurons in the PVH alters food selection, we forcibly expressed the hM3Dq or hM4Di DREADD (a designer receptor exclusively activated by designer drug) (Alexander et al., 2009), respectively, together with the fluorescent protein mCherry (Figure S5F) in CRH neurons of the PVH with the use of transgenic mice expressing Cre recombinase in CRH neurons (CRH-Cre mice). Red fluorescence of mCherry was detected in CRH-positive neurons in the PVH of CRH-Cre:hM3Dq mice (Figure 4A). Application of the hM3Dq agonist clozapine-*N*-oxide (CNO) increased the cytosolic Ca<sup>2+</sup> concentration ([Ca<sup>2+</sup>]<sub>i</sub>) in mCherry-positive CRH neurons, but not in mCherry-negative CRH neurons, isolated from the same animal (Figure 4B). Bilateral injection of CNO into the PVH of CRH-Cre:hM3Dq mice increased selection of HCD1 and reduced that of HFD1 and changed macronutrient intake in a two-diet choice experiment (Figure 4C). Similar to CRH-injected mice (Figure S4B), CRH-Cre:hM3Dq mice injected with CNO fed first on HCD1 (Figure 4C). In contrast, injection of CNO in mice expressing hM4Di in CRH neurons of the PVH (CRH-Cre:hM4Di mice) attenuated the fasting-induced changes in food selection (Figure 4D) and macronutrient intake (Figure S5G). CNO injection also suppressed the fasting-induced increase in c-Fos expression in CRH neurons of the PVH in CRH-Cre:hM4Di mice (Figure 4E). Expression of hM3Dq or hM4Di did not affect selection between HFD1 and HCD1 in the absence of CNO injection (Figures 4C and 4D). Changes in the activity of CRH neurons in the PVH thus altered food selection between an HCD and HFD. Consistent with the anorexic effect of CRH neurons (Arzt and Holsboer, 2006), injection of CNO reduced total calorie intake in CRH-Cre:hM3Dq mice during the initial 3-hr period (saline, 5.7 ± 0.5 kcal; CNO, 3.5 ± 0.3 kcal; p < 0.05), but not the initial 24-hr period after injection (Figure 4C).

We examined the plasma concentration of corticosterone in CRH-Cre:EGFP, CRH-Cre:hM3Dq, CRH-Cre:hM4Di, and CA-AMPK mice. CNO injection into the PVH increased the plasma

### Figure 3. A Subset of CRH Neurons in the PVH Regulates Selection between an HCD and HFD

(A) H&E staining as well as immunohistochemistry analysis of CRH (green) and Thr<sup>172</sup>-phosphorylated AMPK (pAMPK) (red) in the boxed regions of H&E staining for the rostral portion of the PVH in C57BL/6J mice fed *ad libitum* or subjected to an overnight fast with or without refeeding for 3 hr with lab chow. Arrowheads indicate neurons positive for both pAMPK and CRH. Scale bars, 100 μm (H&E staining) or 20 μm (immunofluorescence staining). 3V, third ventricle. See also Figure S4C for pAMPK and CRH staining in the caudal region of the PVH.

(B) qRT-PCR analysis of relative CRH mRNA abundance in the PVH of scramble shRNA or shCRH mice. Data represent means ± SEM (n = 5). \*p < 0.05 versus scramble shRNA mice (left). Representative immunohistochemistry of CRH (green) in the rostral portion of the PVH in scramble shRNA and shCRH mice (right). Scale bar, 50 μm. Higher-magnification views of the boxed regions show individual cells expressing CRH. Scale bar, 10 μm. Endogenous fluorescence of EGFP was lost during paraffin embedding.

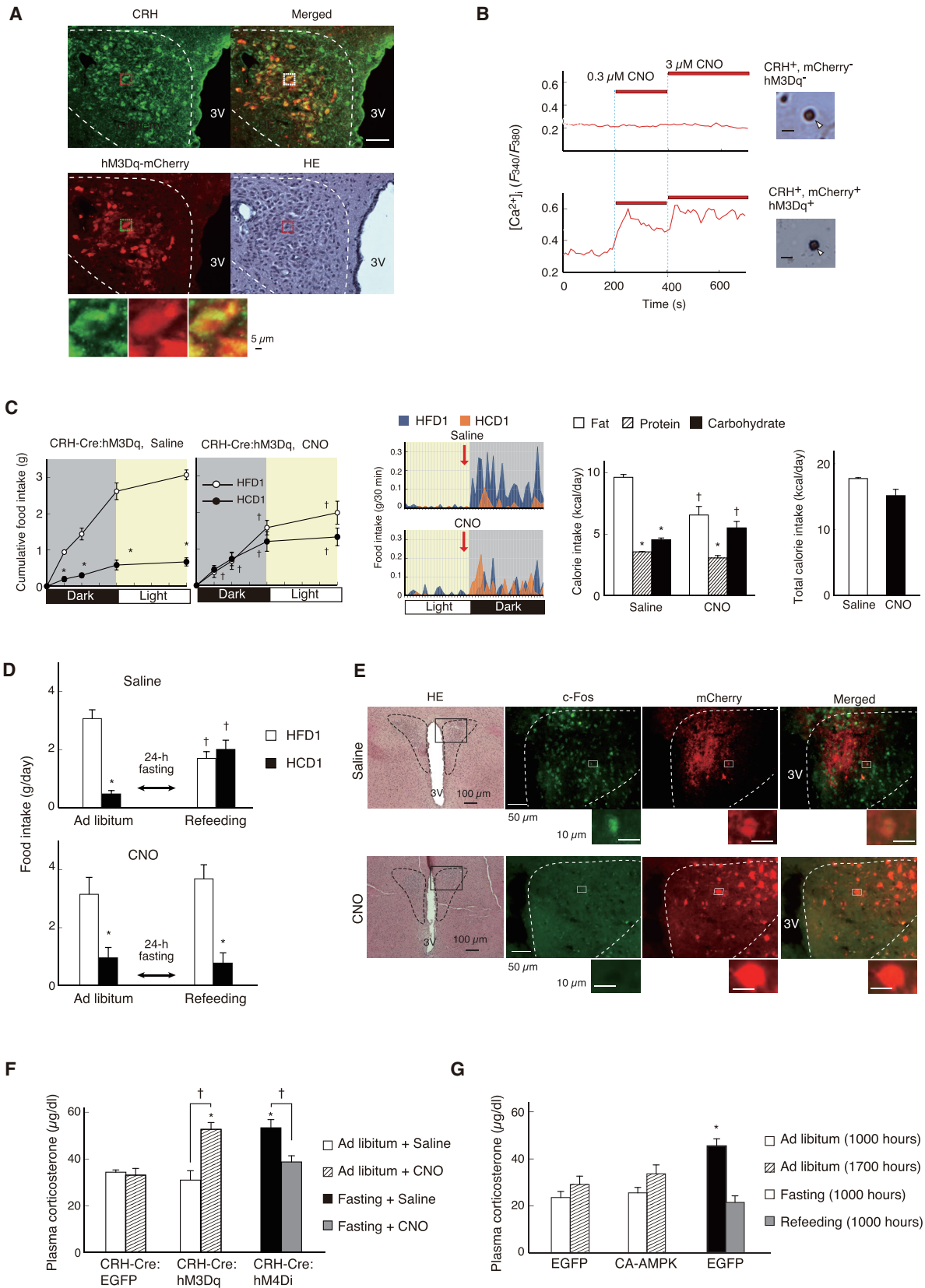
(C) Selection of HFD1 versus HCD1 in a two-diet choice experiment with scramble shRNA and shCRH mice before and after a 24-hr fast. Data represent means ± SEM (n = 5). \*p < 0.05 versus corresponding HFD1 value; †p < 0.05 versus corresponding value for before fasting (*ad libitum*). See also Figure S5C for macronutrient intake in the same mice.

(D) qRT-PCR analysis of relative CRH and CA-AMPK mRNA abundance in the PVH of scramble:CA-AMPK and shCRH:CA-AMPK mice. Data represent means ± SEM (n = 5). \*p < 0.05 versus scramble:CA-AMPK mice.

(E) Selection of HFD1 versus HCD1 in a two-diet choice experiment with scramble:EGFP, scramble:CA-AMPK, shCRH:EGFP, and shCRH:CA-AMPK mice fed *ad libitum*. Data represent means ± SEM (n = 5). \*p < 0.05 versus corresponding HFD1 value; †p < 0.05 versus corresponding value for scramble:EGFP mice. See also Figure S5E for macronutrient intake in the same mice.

(F) Selection of HFD1 versus HCD1 in a two-diet choice experiment performed with scramble:EGFP and shCRH:CA-AMPK mice before and after a 24-hr fast. Data represent means ± SEM (n = 5). \*p < 0.05 versus corresponding HFD1 value; †p < 0.05 versus corresponding value for before fasting (*ad libitum*).

See also Figures S4 and S5.



(legend on next page)

corticosterone levels in CRH-Cre:hM3Dq mice, but not CRH-Cre:EGFP mice, at 10:00 during *ad libitum* feeding with lab chow or after an overnight fast (Figure 4F). Although selection of HCD significantly increased in CA-AMPK mice, the plasma corticosterone levels of CA-AMPK mice at 17:00 (before feeding) as well as 10:00 did not differ from those of EGFP mice (Figure 4G). The plasma corticosterone levels increased in control mice at 10:00 during overnight fast and decreased at 10:00 after refeeding of lab chow for 3 hr (Figure 4G). Thus, plasma corticosterone is unlikely to be a primary mediator of the altered pattern of food selection in CA-AMPK mice, although it might be necessary for control of food intake (Tempel and Leibowitz, 1994).

### AMPK and CPT1c in CRH Neurons Are Necessary for HCD Selection

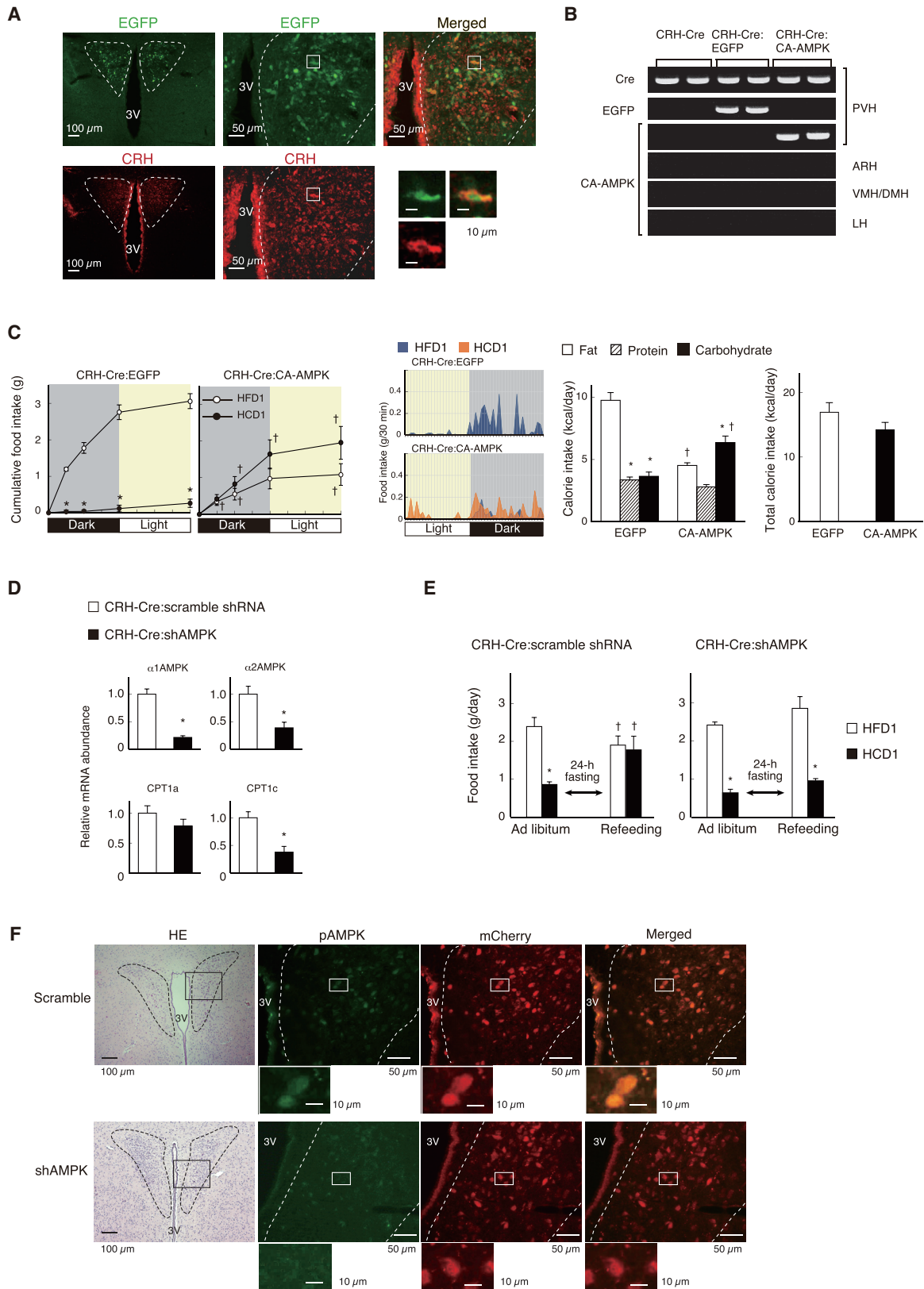
To examine whether AMPK activation in CRH neurons of the PVH is sufficient to change food selection behavior, we introduced a double-floxed construct for CA-AMPK or EGFP (Figure S6A) into the PVH of CRH-Cre mice (to yield CRH-Cre:CA-AMPK and CRH-Cre:EGFP mice, respectively). Immunofluorescence analysis showed that EGFP was coexpressed with CRH in the PVH of CRH-Cre:EGFP mice (Figure 5A). RT-PCR analysis confirmed the production of FLAG-tagged CA-AMPK and EGFP mRNAs in the PVH of CRH-Cre:CA-AMPK and CRH-Cre:EGFP mice, respectively (Figure 5B). CRH-Cre:CA-AMPK mice showed increased selection of HCD1 and reduced selection of HFD1, with corresponding changes in macronutrient intake and without a change in total calorie intake, compared with CRH-Cre:EGFP mice (Figure 5C). Similar to mice injected with CRH (Figure S4B) and CRH-Cre:hM3Dq mice injected with CNO (Figure 4C), CRH-Cre:CA-AMPK mice consumed HCD1 at the beginning of the dark period (Figure 5C). Activation of AMPK in CRH neurons of the PVH is thus sufficient to increase selection for an HCD over an HFD.

To examine whether AMPK in CRH neurons of the PVH is necessary for the fasting-induced change in food selection, we introduced a construct for Cre-dependent expression of AMPK shRNA (Figure S6B) into the PVH of CRH-Cre mice. The resulting CRH-Cre:shAMPK mice showed a reduced abundance of  $\alpha$ 1- and  $\alpha$ 2AMPK and CPT1c mRNAs, but not of CPT1a mRNA, in the PVH compared with CRH-Cre:scramble shRNA control mice (Figure 5D), indicating that AMPK regulates CPT1c mRNA abundance in CRH neurons of the PVH. Fasting-induced changes in both selection of HFD1 versus HCD1 (Figure 5E) and macronutrient uptake (Figure S6C) were attenuated in CRH-Cre:shAMPK mice compared with CRH-Cre:scramble shRNA mice. To confirm that pAMPK abundance is reduced in CRH neurons of the PVH in CRH-Cre:shAMPK mice by immunofluorescence analysis, we introduced constructs that express AMPK shRNA or scramble shRNA and hM4Di-mCherry (as a marker of CRH neurons) in a Cre-dependent manner (Figures S5F and S6B) into the PVH of CRH-Cre mice. The CRH-Cre:shAMPK:hM4Di mice showed a fewer pAMPK-positive CRH neurons of the PVH in the absence of CNO injection (Figure 5F). Together, these results suggested that activation of AMPK in CRH neurons of the PVH is sufficient to induce selection of an HCD over an HFD and is necessary for the fasting-induced change in food selection.

To examine whether the fasting-induced change in food selection behavior also requires CPT1c in CRH neurons of the PVH, we introduced a construct expressing CPT1c shRNA in a Cre-dependent manner (Figure S6B) into the PVH of CRH-Cre mice. The resulting CRH-Cre:shCPT1c mice showed a reduced abundance of CPT1c mRNA, but not of CPT1a mRNA, in the PVH compared with CRH-Cre:scramble shRNA control mice (Figure 6A). This reduction in the amount of CPT1c mRNA was similar to that apparent in CRH-Cre:shAMPK mice (Figure 5D). The fasting-induced changes in selection of HFD1 versus HCD1 (Figure 6B) and in macronutrient intake (Figure S6D)

### Figure 4. Changes in the Activity of CRH Neurons Alter Selection between an HCD and an HFD

- (A) Immunohistofluorescence staining of CRH (green), intrinsic fluorescence of hM3Dq-mCherry (red), and a merged fluorescence image as well as H&E staining for the PVH of CRH-Cre:hM3Dq mice. Scale bar, 50  $\mu$ m. Higher-magnification views of the boxed region show CRH (left), hM3Dq-mCherry (middle), and merged (right) fluorescence signals. Scale bar, 5  $\mu$ m.
- (B) Representative effects of CNO (0.3 or 3  $\mu$ M) on  $[Ca^{2+}]_i$  ( $F_{340}/F_{380}$ ) in isolated CRH-immunoreactive PVH neurons positive or negative for hM3Dq DREADD and mCherry expression. Arrowheads show immunostaining for CRH in the studied neurons. Scale bar, 10  $\mu$ m.
- (C) Selection of HFD1 versus HCD1 in a two-diet choice experiment performed after injection of saline or CNO into the PVH of CRH-Cre:hM3Dq mice 30 min before the onset of the dark period. Cumulative food intake, representative profiles of food intake, macronutrient intake, and 24-hr total calorie intake are shown from left to right. Data represent means  $\pm$  SEM (n = 5). \*p < 0.05 versus corresponding value for HFD1 or fat intake; †p < 0.05 versus corresponding value for saline control.
- (D) Selection of HFD1 versus HCD1 in a two-diet choice experiment performed with CRH-Cre:hM4Di mice either fed *ad libitum* or allowed to refeed after a 24-hr fast. The mice were injected with saline or CNO into the PVH 30 min before measurement of food intake. Data represent means  $\pm$  SEM (n = 5). \*p < 0.05 versus corresponding HFD1 value; †p < 0.05 versus corresponding value for *ad libitum*. See also Figure S5G for macronutrient intake in the same mice.
- (E) Immunohistofluorescence staining for c-Fos (green), intrinsic fluorescence of hM4Di-mCherry (red), and merged fluorescence signals for the boxed regions of H&E staining in the PVH of CRH-Cre:hM4Di mice. Mice were fasted overnight, and c-Fos expression in hM4Di-mCherry-expressing CRH neurons was examined 60 min after CNO or saline injection into the PVH. Scale bars, 100  $\mu$ m (H&E staining) or 50  $\mu$ m (immunofluorescence images). Small lower photos show higher-magnification views of c-Fos, hM4Di-mCherry, and merged fluorescence signals for neurons in the corresponding boxed regions. Scale bars, 10  $\mu$ m. See also Figure S5.
- (F) Plasma corticosterone levels for CRH-Cre:EGFP, CRH-Cre:hM3Dq, and CRH-Cre:hM4Di mice at 10:00 during *ad libitum* feeding with lab chow or after an overnight fast. Data represent means  $\pm$  SEM (n = 5). \*p < 0.05 versus corresponding value in CRH-Cre:EGFP mice; †p < 0.05 versus corresponding value for saline injection. Mice were assayed after maintenance on lab chow for 4 weeks after virus infection.
- (G) Plasma corticosterone levels for EGFP and CA-AMPK mice at 10:00 and 17:00 during *ad libitum* feeding with lab chow or at 10:00 after an overnight fast with or without refeeding for 3 hr. Data represent means  $\pm$  SEM (n = 6). \*p < 0.05 versus value for EGFP mice at 10:00 during *ad libitum* feeding. Mice were assayed after maintenance on lab chow for 4 weeks after virus infection.



(legend on next page)

were also attenuated in CRH-Cre:shCPT1c mice to an extent similar to that in CRH-Cre:shAMPK mice (Figures 5E and S6C). We again confirmed by immunofluorescence analysis that the abundance of CPT1c was reduced in CRH neurons of the PVH in CRH-Cre:shCPT1c mice (Figure 6C) with the use of constructs that express CPT1c shRNA and hM4Di-mCherry in a Cre-dependent manner (Figures S5F and S6B). Together, these results suggested that the AMPK-CPT1c axis in CRH neurons of the PVH is necessary for the fasting-induced increase in selection of an HCD over an HFD.

### AMPK and CPT1c Regulate $[Ca^{2+}]_i$ in CRH Neurons

CPT1c is localized to the endoplasmic reticulum (ER) (Sierra et al., 2008) and mitochondria (Dai et al., 2007). We examined the effect of the AMPK activator AICAR on  $[Ca^{2+}]_i$  in CRH neurons isolated from the PVH. AICAR increased  $[Ca^{2+}]_i$  in CRH-positive (CRH<sup>+</sup>, EGFP<sup>+</sup>, scramble shRNA<sup>+</sup>) neurons (Figure 7A). The CPT1 inhibitor etomoxir inhibited the  $Ca^{2+}$  response to AICAR in AICAR-responsive CRH neurons, whereas it did not inhibit the KCl-induced increase in  $[Ca^{2+}]_i$  in CRH neurons (Figure 7B, top panel). CRH neurons expressing AMPK shRNA (CRH<sup>+</sup>, EGFP<sup>+</sup>, and shAMPK<sup>+</sup>) or CPT1c shRNA (CRH<sup>+</sup>, EGFP<sup>+</sup>, and shCPT1c<sup>+</sup>) that were isolated from the PVH did not show a  $Ca^{2+}$  response to AICAR but did respond to KCl (Figure 7B), indicating that AICAR increases  $[Ca^{2+}]_i$  in CRH neurons of the PVH via activation of AMPK and CPT1c. Activation of the AMPK-CPT1c axis thus results in an increase in  $[Ca^{2+}]_i$  in CRH neurons of the PVH.

## DISCUSSION

We have shown that activation of AMPK in a subset of CRH neurons in the PVH is sufficient for selection between an HCD and an HFD. Fasting resulted in increased HCD intake and reduced HFD intake through activation of AMPK in CRH neurons of the rostral region of the PVH. Our results reveal that these CRH neurons serve as “food selection” neurons that release CRH in the PVH to trigger the choice of an HCD during refeeding after fasting, with the preference for sweet and fat tastes being unaffected.

Consumption of an HCD results in a rapid improvement in ketone body metabolism in fasted mice. Thus, selection of an HCD by activation of AMPK in a subset of CRH neurons may have a beneficial role to quickly normalize ketone and glucose metabolism in mice during refeeding after fasting. Given that diuretic hormone 44 (Dh44), a *Drosophila* ortholog of mammalian CRH, contributes to nutritive sugar selection (Dus et al., 2015), CRH-induced carbohydrate selection might be conserved from insects to mammals.

To identify the principle neuron for carbohydrate selection, we first injected peptides or proteins expressed in the PVH into the lateral ventricle (Figure S4), but no peptide or protein increased carbohydrate selection. Oxytocin has been shown to be released from the dendrites and cell body (Jin et al., 2007). We therefore next injected the peptides and proteins into the PVH, and only CRH injection into the PVH increased carbohydrate selection. Thus, CRH may be released into the PVH in a paracrine manner, regulate other PVH neurons, and increase selection of carbohydrate over fat.

We found that fasting-induced activation of AMPK in CRH neurons of the PVH triggers a pathway that leads to an increase in  $[Ca^{2+}]_i$  in these neurons, which is necessary for induction of HCD selection behavior. Activation of AMPK inhibits ACC, resulting in a reduced abundance of malonyl-CoA and leading to activation of CPT1c in these CRH neurons. In contrast to CPT1a, CPT1c is localized to the ER (Sierra et al., 2008) and mitochondria (Dai et al., 2007), and both of these organelles contribute to intracellular  $Ca^{2+}$  signaling in a cooperative manner (Pizzo and Pozzan, 2007). Activation of the AMPK-CPT1c axis thus triggers an oscillatory  $[Ca^{2+}]_i$  response in CRH neurons via  $Ca^{2+}$  release from the ER or mitochondria in cooperation with its effect on FAO, resulting in increased synaptic activity in these neurons and HCD selection. CPT1a in CRH neurons may also be involved in AMPK-induced selection of HCD over HFD. Further investigation is needed to determine whether FAO induced by CPT1a regulates  $[Ca^{2+}]_i$  response in CRH neurons and food selection.

The activation of AMPK in CRH neurons of the PVH by food deprivation was attenuated by 3 hr of refeeding with HCD, whereas HCD intake continued for up to 24 hr, suggesting that

### Figure 5. AMPK in CRH Neurons Regulates Selection between an HCD and an HFD

(A) Immunohistofluorescence staining of CRH (red), intrinsic fluorescence of EGFP (green), and merged fluorescence images for the PVH of CRH-Cre:EGFP mice. Scale bars, 100  $\mu$ m (left) and 50  $\mu$ m (middle and right). Higher-magnification views of the boxed regions show EGFP (top left), CRH (bottom left), and merged (top right) images. Scale bar, 10  $\mu$ m.

(B) RT-PCR analysis of Cre recombinase, EGFP, and CA-AMPK mRNAs in the PVH, ARH, VMH/DMH, and LH of CRH-Cre:EGFP and CRH-Cre:CA-AMPK mice at 4 weeks after lentivirus infection as well as in noninfected CRH-Cre mice.

(C) Selection of HFD1 versus HCD1 in a two-diet choice experiment with CRH-Cre:EGFP and CRH-Cre:CA-AMPK mice. Cumulative food intake, representative profiles of food intake, macronutrient intake, and 24-hr total calorie intake are shown from left to right. Data represent means  $\pm$  SEM (n = 8). \*p < 0.05 versus corresponding value for HFD1 or fat intake; †p < 0.05 versus corresponding value for CRH-Cre:EGFP mice.

(D) qRT-PCR analysis of relative  $\alpha$ 1- and  $\alpha$ 2AMPK, CPT1a, and CPT1c mRNA abundance in the PVH of CRH-Cre:scramble shRNA or CRH-Cre:shAMPK mice that had been deprived of food overnight. Data represent means  $\pm$  SEM (n = 6). \*p < 0.05 versus corresponding value for CRH-Cre:scramble shRNA mice.

(E) Selection of HFD1 versus HCD1 in a two-diet choice experiment performed with CRH-Cre:scramble shRNA and CRH-Cre:shAMPK mice before and after a 24-hr fast. Data represent means  $\pm$  SEM (n = 6). \*p < 0.05 versus corresponding HFD1 value; †p < 0.05 versus corresponding value for *ad libitum*. See also Figure S6C for macronutrient intake in the same mice.

(F) Immunohistofluorescence analysis of Thr<sup>172</sup>-phosphorylated AMPK (pAMPK) (green), intrinsic fluorescence of hM4Di-mCherry (red, marker for CRH neurons), and merged fluorescence images for the boxed regions of H&E staining in the rostral portion of the PVH in CRH-Cre:scramble shRNA:hM4Di and CRH-Cre:shAMPK:hM4Di mice subjected to an overnight fast. Scale bars represent 100  $\mu$ m (H&E staining) or 50  $\mu$ m (fluorescence images). Higher-magnification views of the boxed regions in the fluorescence images are shown below. Scale bars, 10  $\mu$ m. Endogenous fluorescence of EGFP encoded by the lentivirus vector was lost during paraffin embedding.

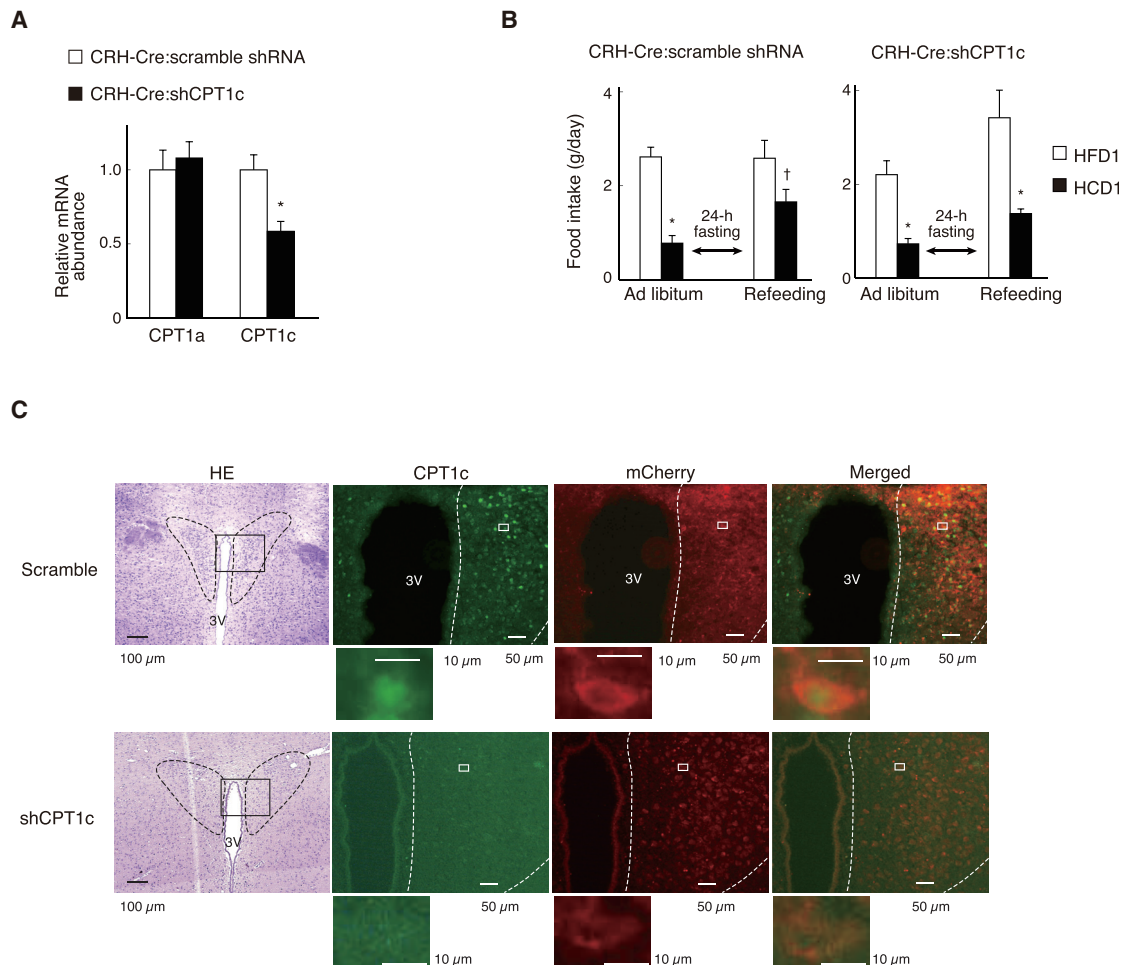


**Figure 6. CPT1c in CRH Neurons Regulates Selection between an HCD and an HFD**

(A) qRT-PCR analysis of relative CPT1a and CPT1c mRNA abundance in the PVH of CRH-Cre:scramble shRNA or CRH-Cre:shCPT1c mice that had been deprived of food overnight. Data represent means  $\pm$  SEM (n = 7). \*p < 0.05 versus corresponding value for CRH-Cre:scramble shRNA mice.

(B) Selection of HFD1 versus HCD1 in a two-diet choice experiment performed with CRH-Cre:scramble shRNA and CRH-Cre:shCPT1c mice before and after a 24-hr fast. Data represent means  $\pm$  SEM (n = 6). \*p < 0.05 versus corresponding HFD1 value; †p < 0.05 versus corresponding value for *ad libitum*. See also Figure S6D for macronutrient intake in the same mice.

(C) Immunohistochemistry analysis of CPT1c (green), intrinsic fluorescence of hM4Di-mCherry (red, marker for CRH neurons), and merged fluorescence images for the boxed regions of H&E staining in the rostral portion of the PVH in CRH-Cre:scramble shRNA:hM4Di and CRH-Cre:shCPT1c:hM4Di mice subjected to an overnight fast. Scale bars, 100  $\mu$ m (H&E staining) and 50  $\mu$ m (fluorescence images). Higher-magnification views of neurons in the boxed regions of the fluorescence images are shown below. Scale bar, 10  $\mu$ m. Endogenous fluorescence of EGFP encoded by the lentivirus vector was lost during paraffin embedding. See also Figure S6.

AMPK activation in these neurons during fasting serves as the initiator for HCD selection. Similarly, activation of neuropeptide Y (NPY)- and Agouti-related peptide (AgRP)-expressing neurons in the ARH during fasting is rapidly suppressed by refeeding, whereas the effect on feeding continues over 24 hr (Betley et al., 2015; Yang et al., 2011). Activation of AMPK is essential for the fasting-induced change in plasticity of AgRP neurons in the ARH at both presynaptic and postsynaptic levels (Kong et al., 2016; Yang et al., 2011). CPT1c regulates expression of the  $\alpha$ -amino-3-hydroxy-5-methyl-4-isoxazole propionic acid (AMPA) receptor subunit GluA1 in hippocampal neurons (Fadó et al., 2015). AMPK may therefore regulate neuronal plasticity in CRH neurons through activation of CPT1c and an increase

in  $[Ca^{2+}]_i$ . In addition, we have previously shown that increased glucose level in the brain inhibits AMPK activity in the PVH (Minokoshi et al., 2004). Furthermore, AMPK activates CPT1c via suppression of ACC and a decrease in malonyl-CoA content. Increased glucose levels in the brain may result in higher malonyl-CoA levels in CRH neurons and inhibition of CPT1c activity. Thus, the AMPK-CPT1c system in CRH neurons provides the mechanism by which refeeding of HCD after fasting inhibits CRH neurons and selection of carbohydrate over fat.

Perception of sweet taste and an HFD induces hedonic feeding in rodents. However, a change in sweet taste sensing is unlikely the primary mediator of fasting-induced HCD selection, given that injection of etomoxir into the PVH did not affect

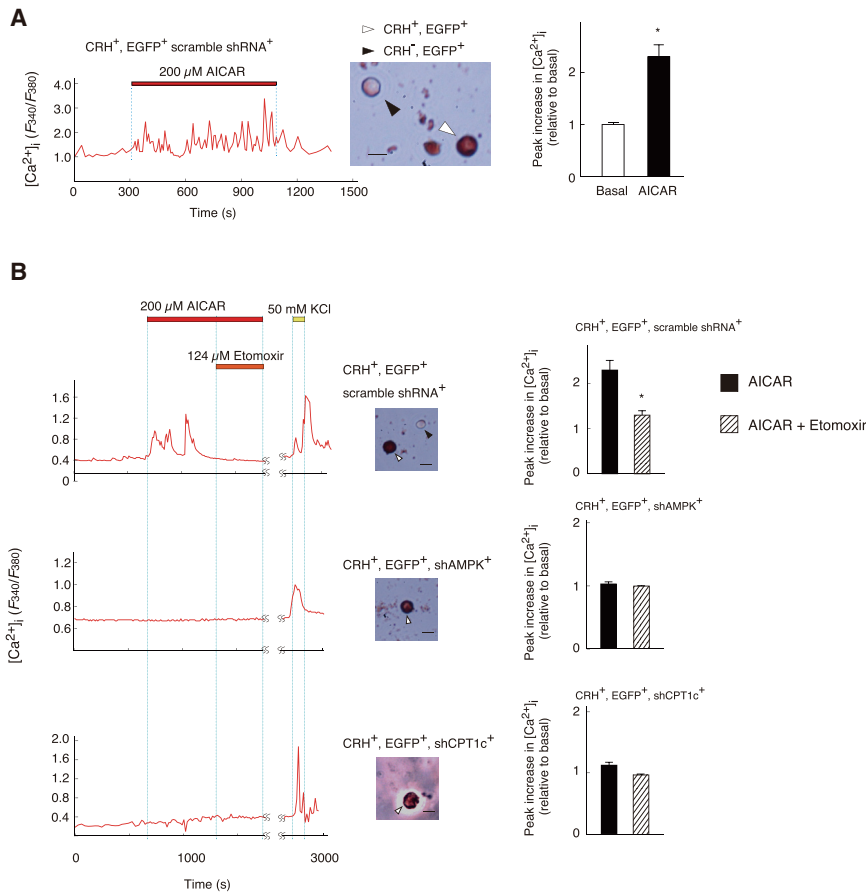


**Figure 7. AMPK Activation Increases  $[Ca^{2+}]_i$  in CRH Neurons**

(A) Effect of AICAR (200  $\mu$ M) on  $[Ca^{2+}]_i$  in CRH-positive PVH neurons expressing a scrambled shRNA and EGFP that were isolated from CRH-Cre:scramble shRNA mice. A representative  $[Ca^{2+}]_i$  trace is shown in the left panel. Immunostaining for CRH in the studied CRH-positive and EGFP-fluorescence-positive (marker of shRNA expression) neuron indicated by the white arrowhead is shown in the middle panel; the black arrowhead indicates a CRH-negative and EGFP-fluorescence-positive neuron, and the scale bar represents 10  $\mu$ m. The maximal increase in  $[Ca^{2+}]_i$  induced by AICAR (200  $\mu$ M) determined for seven AICAR-responsive, CRH-positive, and EGFP-fluorescence-positive neurons is shown in the right panel; data represent means  $\pm$  SEM (\* $p < 0.05$  versus the basal value).

(B) Effects of AICAR, etomoxir, and KCl on  $[Ca^{2+}]_i$  in isolated CRH-positive PVH neurons expressing scrambled, AMPK, or CPT1c shRNAs. Representative effects of AICAR, etomoxir, and KCl are shown together with immunostaining for CRH in the studied CRH-positive, EGFP-fluorescence-positive neurons (white arrowheads). Black arrowheads indicate CRH-negative, EGFP-positive neurons isolated from the same mice. Scale bars, 10  $\mu$ m. The maximal increases in  $[Ca^{2+}]_i$  induced by AICAR in the absence or presence of etomoxir determined for 10 AICAR-responsive, CRH-positive, EGFP-positive neurons expressing the scrambled, AMPK, or CPT1c shRNAs are also shown. Data represent means  $\pm$  SEM. \* $p < 0.05$  versus AICAR alone.

the amount of saccharin solution consumed by mice. Preference for an HFD is also maintained during fasting, as evidenced by our observation that mice initially ate an HFD before switching to an HCD. Furthermore, fasted mice showed an increased intake of an HFD compared with an HCD when the diets were presented alone. AMPK-induced HCD selection is thus not likely mediated by changes in the perception of sweet and fat taste. Metabolic changes in the brain and peripheral tissues during fasting may serve as the signal initiating HCD selection, given that injection of glucose into the lateral ventricle, which inhibits activation of AMPK in the PVH by food deprivation (Minokoshi et al., 2004), suppressed HCD selection and increased HFD selection during refeeding after fasting. We found that the plasma corticosterone level is also unlikely to be the primary regulator of such food selection behavior. Our results suggest that CRH neurons have three distinct functions: (1) regulation of the plasma corticosterone level, (2) suppression of total calorie intake, and (3) selection of carbohydrate over fat.

Injection of NPY into the PVH increases carbohydrate feeding (Leibowitz, 1995), food deprivation activates NPY/AgRP neurons in the ARH (Stenerson, 2013), and CRH neurons in the PVH are activated by NPY (Dimitrov et al., 2007), although NPY receptors are coupled to inhibitory G proteins (Drakulich et al., 2003). A subset of CRH neurons is innervated by  $\gamma$ -aminobutyric acid (GABA)-positive neurons (Miklós and Kovács, 2002), and NPY in-

hibits GABA<sub>A</sub>-receptor-mediated synaptic transmission in the PVH (Cowley et al., 1999). NPY therefore likely activates AMPK in a subset of CRH neurons in the PVH by inhibiting GABAergic neurons. Characterization of the pathways upstream and downstream of CRH neurons may lead to identification of the molecular mechanisms that determine food selection behavior under physiological and pathological conditions.

Dysregulation of food selection behavior is associated with stressful life events in humans (Roberts et al., 2014; Rutters et al., 2009). CRH neurons in the PVH are activated by stress (Elliott et al., 2010). Thus, stress may activate AMPK in a subset of CRH neurons and induce selection of an HCD, such as sweet foods. Further characterization of AMPK signaling in CRH neurons of the PVH might therefore result in a better understanding of the molecular mechanisms underlying the effects of stress and obesity on food selection behavior.

## EXPERIMENTAL PROCEDURES

### Animals

Male C57BL/6J mice were obtained from Nihon SLC (Hamamatsu, Japan) and male CRH-Cre transgenic mice from The Jackson Laboratory (Bar Harbor, ME). Most mice were studied at 10 to 14 weeks of age, and virus-infected mice were studied 4 weeks after infection. Mice were housed individually in plastic cages at 24°C  $\pm$  1°C and with lights on from 06:00 to 18:00. Some mice were preimplanted bilateral guide cannula stereotaxically and bilaterally

into the PVH or unilaterally into the lateral ventricle according to the atlas of Paxinos and Franklin (1997), as described previously (Shiuchi et al., 2009). Additional details for animals and surgical procedures are described in Supplemental Experimental Procedures.

### Viral Infection of the PVH

Mice with a preimplanted bilateral guide cannula in the PVH were anesthetized, and 400 nL of the virus stock suspension ( $2.5 \times 10^9$  transducing units [TUs]/mL) was infused at a flow rate of 50 nL/min bilaterally into the PVH with the use of an infusion pump. Additional details for virus production, viral infection of the PVH, and administration of agents into the PVH or lateral ventricle are in Supplemental Experimental Procedures.

### Measurement of Food Selection

Food selection and water drinking were measured with a multifaceted feeding and activity monitoring system (MFD-100M; Shinfactory, Fukuoka, Japan; Figure 1F). For examination of food selection after food deprivation, both the HCD and the HFD were removed for a 24-hr period (from 17:30 to 18:00) on the experimental day. CRH and other agents were injected into the PVH bilaterally or i.c.v. through the preimplanted cannula at 17:30 on the day of the experiment. Food selection was monitored every minute, and cumulative data for each 30-min period were analyzed. Additional details for measurements of food selection, saccharin, water drinking, and energy expenditure are in Supplemental Experimental Procedures.

### FAO in the PVH *Ex Vivo*

For examination of the effect of etomoxir on the fasting-induced change in FAO in the PVH, etomoxir was injected unilaterally into one side of the PVH (3 nmol). Immediately after removal of the brain, each side of the PVH was then harvested with the use of a punched-out needle. The side of the PVH injected with etomoxir was incubated in the additional presence of etomoxir (60  $\mu$ M). FAO was calculated as femtomoles of the  $^3\text{H}_2\text{O}$  produced from 9,10- $^3\text{H}$ palmitic acid per hour and per unilateral side of the PVH, respectively. Details regarding measurements of FAO, AMPK activity, and blood metabolites and qRT-PCR, immunostaining, and immunoblotting are in Supplemental Experimental Procedures.

### Identification of AICAR-Responsive CRH Neurons in the PVH

Single neurons were prepared from the PVH substantially as described previously (Maejima et al., 2009). After  $[\text{Ca}^{2+}]_i$  measurements, single neurons were fixed in 4% paraformaldehyde and then subjected to immunostaining for CRH, as previously described. Additional details are in Supplemental Experimental Procedures.

### Statistics

Data are presented as means  $\pm$  SEM and were compared using ANOVA followed by the Tukey post hoc test or an unpaired or paired Student's *t* test (two tailed). To analyze the results of energy expenditure, the data were also compared by analysis of covariance (ANCOVA) with body weight of mice. A *p* value of  $< 0.05$  was considered statistically significant.

### SUPPLEMENTAL INFORMATION

Supplemental information includes Supplemental Experimental Procedures, six figures, three tables, and one movie and can be found with this article online at <https://doi.org/10.1016/j.celrep.2017.11.102>.

A video abstract is available at <https://doi.org/10.1016/j.celrep.2017.11.102#mmc4>.

### ACKNOWLEDGMENTS

We thank Y. Kubo for advice and discussion, P. Osten and B. Roth for viral vectors, M. Hayashi for help with manuscript preparation, R. Kageyama for virus preparation, the Functional Genomics Facility at the National Institute for Basic Biology (NIBB) for DNA sequencing, and the Center for Radioisotope Facilities at the NIBB for performing radioisotope experiments. This study was sup-

ported by Grants-in-Aid for Scientific Research (B) (16390062, 19390059, 21390067, and 24390058 to Y. Minokoshi), Grants-in-Aid for Exploratory Research (17659069 and 15K15352 to Y. Minokoshi), a Grant-in-Aid for Scientific Research on Innovative Areas (22126005 to Y. Minokoshi), Grants-in-Aid for Young Scientists (B) (18790629, 20790656, and 22790875 to S.O.), and Grants-in-Aid for Scientific Research (C) (24591374 and 15K09405 to S.O.) from the Ministry of Education, Culture, Sports, Science, and Technology of Japan and the Japan Society for the Promotion of Science. B.B.K. is supported by the NIH (grant R01 DK043051) and the JPB Foundation.

### AUTHOR CONTRIBUTIONS

S.O. constructed viral vectors and performed animal studies, FAO measurements, immunohistochemistry, immunofluorescence analysis for DREADD, and PCR, immunoblot, blood metabolite, and statistical analyses and contributed to  $\text{Ca}^{2+}$  imaging for shAMPK and shCPT1c mice. T. Sato contributed to animal studies. M.T. performed  $\text{Ca}^{2+}$  imaging for shAMPK and shCPT1c mice. H.K. performed immunofluorescence analysis for pAMPK and CRH. Y. Maejima, M. Nakata, U.S., and B.Z. performed  $\text{Ca}^{2+}$  imaging for AICAR. S.H. contributed to immunofluorescence analysis for pAMPK and CRH. T.M. contributed to animal studies for CA-AMPK mice. S.K. contributed to measurement of plasma corticosterone. T. Shiuchi supervised feeding analysis. C.T. contributed to measurement of AMPK activity. K.S. contributed to maintenance of mouse lines. N.F.A. and S.Y. contributed to immunoblot analysis. K.K. prepared viral vectors. F.F. and P.F. prepared the CA-AMPK construct. T.Y. supervised  $\text{Ca}^{2+}$  imaging for AICAR. S.S. supervised immunofluorescence analysis for pAMPK and CRH. H.M. and M. Nakazato supervised the project. B.B.K. supervised the project and edited the manuscript. Y. Minokoshi supervised and coordinated the project and wrote the manuscript with the support of S.O.

### DECLARATION OF INTERESTS

The authors declare no competing interests.

Received: August 4, 2017

Revised: October 28, 2017

Accepted: November 29, 2017

Published: January 16, 2018

### REFERENCES

- Alexander, G.M., Rogan, S.C., Abbas, A.I., Armbruster, B.N., Pei, Y., Allen, J.A., Nonneman, R.J., Hartmann, J., Moy, S.S., Nicoletis, M.A., et al. (2009). Remote control of neuronal activity in transgenic mice expressing evolved G protein-coupled receptors. *Neuron* 63, 27–39.
- Andrews, Z.B., Liu, Z.W., Wallingford, N., Erion, D.M., Borok, E., Friedman, J.M., Tschöp, M.H., Shanabrough, M., Cline, G., Shulman, G.I., et al. (2008). UCP2 mediates ghrelin's action on NPY/AgRP neurons by lowering free radicals. *Nature* 454, 846–851.
- Arzt, E., and Holsboer, F. (2006). CRF signaling: molecular specificity for drug targeting in the CNS. *Trends Pharmacol. Sci.* 27, 531–538.
- Bentebibel, A., Sebastián, D., Herrero, L., López-Viñas, E., Serra, D., Asins, G., Gómez-Puertas, P., and Hegardt, F.G. (2006). Novel effect of C75 on carnitine palmitoyltransferase I activity and palmitate oxidation. *Biochemistry* 45, 4339–4350.
- Betley, J.N., Xu, S., Cao, Z.F.H., Gong, R., Magnus, C.J., Yu, Y., and Sternson, S.M. (2015). Neurons for hunger and thirst transmit a negative-valence teaching signal. *Nature* 521, 180–185.
- Cheng, Y., Zhang, Q., Meng, Q., Xia, T., Huang, Z., Wang, C., Liu, B., Chen, S., Xiao, F., Du, Y., and Guo, F. (2011). Leucine deprivation stimulates fat loss via increasing CRH expression in the hypothalamus and activating the sympathetic nervous system. *Mol. Endocrinol.* 25, 1624–1635.
- Cowley, M.A., Pronchuk, N., Fan, W., Dinulescu, D.M., Colmers, W.F., and Cone, R.D. (1999). Integration of NPY, AGRP, and melanocortin signals in

- the hypothalamic paraventricular nucleus: evidence of a cellular basis for the adipostat. *Neuron* 24, 155–163.
- Dai, Y., Wolfgang, M.J., Cha, S.H., and Lane, M.D. (2007). Localization and effect of ectopic expression of CPT1c in CNS feeding centers. *Biochem. Biophys. Res. Commun.* 359, 469–474.
- Dimitrov, E.L., DeJoseph, M.R., Brownfield, M.S., and Urban, J.H. (2007). Involvement of neuropeptide Y Y1 receptors in the regulation of neuroendocrine corticotropin-releasing hormone neuronal activity. *Endocrinology* 148, 3666–3673.
- Drakulich, D.A., Walls, A.M., Toews, M.L., and Hexum, T.D. (2003). Neuropeptide Y receptor-mediated sensitization of ATP-stimulated inositol phosphate formation. *J. Pharmacol. Exp. Ther.* 307, 559–565.
- Dus, M., Lai, J.S., Gunapala, K.M., Min, S., Tayler, T.D., Hergarden, A.C., Geraud, E., Joseph, C.M., and Suh, G.S. (2015). Nutrient sensor in the brain directs the action of the brain-gut axis in *Drosophila*. *Neuron* 87, 139–151.
- Elliott, E., Ezra-Nevo, G., Regev, L., Neufeld-Cohen, A., and Chen, A. (2010). Resilience to social stress coincides with functional DNA methylation of the *Crf* gene in adult mice. *Nat. Neurosci.* 13, 1351–1353.
- Enerbäck, S., Jacobsson, A., Simpson, E.M., Guerra, C., Yamashita, H., Harper, M.E., and Kozak, L.P. (1997). Mice lacking mitochondrial uncoupling protein are cold-sensitive but not obese. *Nature* 387, 90–94.
- Fadó, R., Soto, D., Miñano-Molina, A.J., Pozo, M., Carrasco, P., Yefimenko, N., Rodríguez-Álvarez, J., and Casals, N. (2015). Novel regulation of the synthesis of alpha-amino-3-hydroxy-5-methyl-4-isoxazolepropionic acid (AMPA) receptor subunit GluA1 by carnitine palmitoyltransferase 1c (CPT1C) in the hippocampus. *J. Biol. Chem.* 290, 25548–25560.
- Hardie, D.G. (2007). AMP-activated/SNF1 protein kinases: conserved guardians of cellular energy. *Nat. Rev. Mol. Cell Biol.* 8, 774–785.
- Hunsicker, K.D., Mullen, B.J., and Martin, R.J. (1992). Effect of starvation or restriction on self-selection of macronutrients in rats. *Physiol. Behav.* 51, 325–330.
- Jin, D., Liu, H.X., Hirai, H., Torashima, T., Nagai, T., Lopatina, O., Shnyder, N.A., Yamada, K., Noda, M., Seike, T., et al. (2007). CD38 is critical for social behaviour by regulating oxytocin secretion. *Nature* 446, 41–45.
- Kim, E.K., Miller, I., Aja, S., Landree, L.E., Pinn, M., McFadden, J., Kuhajda, F.P., Moran, T.H., and Ronnett, G.V. (2004). C75, a fatty acid synthase inhibitor, reduces food intake via hypothalamic AMP-activated protein kinase. *J. Biol. Chem.* 279, 19970–19976.
- Kong, D., Dagon, Y., Campbell, J.N., Guo, Y., Yang, Z., Yi, X., Aryal, P., Wellenstein, K., Kahn, B.B., Sabatini, B.L., and Lowell, B.B. (2016). A postsynaptic AMPK→p21-activated kinase pathway drives fasting-induced synaptic plasticity in AgRP neurons. *Neuron* 91, 25–33.
- Leibowitz, S.F. (1995). Brain peptides and obesity: pharmacologic treatment. *Obes. Res.* 3 (Suppl 4), 573S–589S.
- Loftus, T.M., Jaworsky, D.E., Frehywot, G.L., Townsend, C.A., Ronnett, G.V., Lane, M.D., and Kuhajda, F.P. (2000). Reduced food intake and body weight in mice treated with fatty acid synthase inhibitors. *Science* 288, 2379–2381.
- López, M., Lage, R., Saha, A.K., Pérez-Tilve, D., Vázquez, M.J., Varela, L., Sangiao-Alvarellos, S., Tovar, S., Raghay, K., Rodríguez-Cuenca, S., et al. (2008). Hypothalamic fatty acid metabolism mediates the orexigenic action of ghrelin. *Cell Metab.* 7, 389–399.
- Maejima, Y., Sedbazar, U., Suyama, S., Kohno, D., Onaka, T., Takano, E., Yoshida, N., Koike, M., Uchiyama, Y., Fujiwara, K., et al. (2009). Nesfatin-1-regulated oxytocinergic signaling in the paraventricular nucleus causes anorexia through a leptin-independent melanocortin pathway. *Cell Metab.* 10, 355–365.
- Mann, J.I. (2002). Diet and risk of coronary heart disease and type 2 diabetes. *Lancet* 360, 783–789.
- Miklós, I.H., and Kovács, K.J. (2002). GABAergic innervation of corticotropin-releasing hormone (CRH)-secreting parvocellular neurons and its plasticity as demonstrated by quantitative immunoelectron microscopy. *Neuroscience* 113, 581–592.
- Minokoshi, Y., Alquier, T., Furukawa, N., Kim, Y.B., Lee, A., Xue, B., Mu, J., Fofelle, F., Ferré, P., Birnbaum, M.J., et al. (2004). AMP-kinase regulates food intake by responding to hormonal and nutrient signals in the hypothalamus. *Nature* 428, 569–574.
- Paxinos, G., and Franklin, K.B.J. (1997). *The Mouse Brain in Stereotaxic Coordinates* (Academic Press).
- Pizzo, P., and Pozzan, T. (2007). Mitochondria-endoplasmic reticulum choreography: structure and signaling dynamics. *Trends Cell Biol.* 17, 511–517.
- Roberts, C.J., Campbell, I.C., and Troop, N. (2014). Increases in weight during chronic stress are partially associated with a switch in food choice towards increased carbohydrate and saturated fat intake. *Eur. Eat. Disord. Rev.* 22, 77–82.
- Rutters, F., Nieuwenhuizen, A.G., Lemmens, S.G., Born, J.M., and Westerterp-Plantenga, M.S. (2009). Acute stress-related changes in eating in the absence of hunger. *Obesity (Silver Spring)* 17, 72–77.
- Shiuchi, T., Haque, M.S., Okamoto, S., Inoue, T., Kageyama, H., Lee, S., Toda, C., Suzuki, A., Bachman, E.S., Kim, Y.B., et al. (2009). Hypothalamic orexin stimulates feeding-associated glucose utilization in skeletal muscle via sympathetic nervous system. *Cell Metab.* 10, 466–480.
- Sierra, A.Y., Gratacós, E., Carrasco, P., Clotet, J., Ureña, J., Serra, D., Asins, G., Hegardt, F.G., and Casals, N. (2008). CPT1c is localized in endoplasmic reticulum of neurons and has carnitine palmitoyltransferase activity. *J. Biol. Chem.* 283, 6878–6885.
- Sternson, S.M. (2013). Hypothalamic survival circuits: blueprints for purposive behaviors. *Neuron* 77, 810–824.
- Tellez, L.A., Han, W., Zhang, X., Ferreira, T.L., Perez, I.O., Shammah-Lagnado, S.J., van den Pol, A.N., and de Araujo, I.E. (2016). Separate circuitries encode the hedonic and nutritional values of sugar. *Nat. Neurosci.* 19, 465–470.
- Tempel, D.L., and Leibowitz, S.F. (1994). Adrenal steroid receptors: interactions with brain neuropeptide systems in relation to nutrient intake and metabolism. *J. Neuroendocrinol.* 6, 479–501.
- Welch, C.C., Grace, M.K., Billington, C.J., and Levine, A.S. (1994). Preference and diet type affect macronutrient selection after morphine, NPY, norepinephrine, and deprivation. *Am. J. Physiol.* 266, R426–R433.
- Woods, A., Azzout-Marniche, D., Foretz, M., Stein, S.C., Lemarchand, P., Ferré, P., Fofelle, F., and Carling, D. (2000). Characterization of the role of AMP-activated protein kinase in the regulation of glucose-activated gene expression using constitutively active and dominant negative forms of the kinase. *Mol. Cell Biol.* 20, 6704–6711.
- Wortman, M.D., Clegg, D.J., D'Alessio, D., Woods, S.C., and Seeley, R.J. (2003). C75 inhibits food intake by increasing CNS glucose metabolism. *Nat. Med.* 9, 483–485.
- Yang, Y., Atasoy, D., Su, H.H., and Sternson, S.M. (2011). Hunger states switch a flip-flop memory circuit via a synaptic AMPK-dependent positive feedback loop. *Cell* 146, 992–1003.